

Numerical investigation of a new LH2 centrifugal pump concept used in space propulsion

Ion MALAEL*¹, George Bogdan GHERMAN¹, Ionut PORUMBEL¹

*Corresponding author

¹National Research and Development Institute for Gas Turbines COMOTI, 220 D Iuliu Maniu Bd., sector 6, cod 061126, OP 76, CP174, Bucharest, Romania, ion.malael@comoti.ro*, bogdan.gherman@comoti.ro, ionut.porumbel@comoti.ro

DOI: 10.13111/2066-8201.2018.10.2.7

Received: 10 January 2018/ Accepted: 22 January 2018/ Published: June 2018

Copyright © 2018. Published by INCAS. This is an “open access” article under the CC BY-NC-ND license (<http://creativecommons.org/licenses/by-nc-nd/4.0/>)

Aerospace Europe CEAS 2017 Conference,

16th-20th October 2017, Palace of the Parliament, Bucharest, Romania

Technical session Space Propulsion

Abstract: *The present study deals with efficiency increase of a centrifugal pump for liquid rocket propulsion by using an innovative concept. With this new pump design the axial length will be reduced by 60% and 20% mass weight towards a classic two stage centrifugal pump. To estimate the performances, the CFD methods were used. The CFD analysis will be performed on 3D domains with the CFD commercial code ANSYS CFX. The numerical solvers used are pressure based with the SIMPLE method for RANS. The domain discretization was done by using dedicated grid generators like TurboGrid and ICEM CFD. The results were compared with a classic configuration with two stages in series. Centrifugal pump characteristics, such as pressure inlet-outlet variation, velocity and streamline patterns are presented in the paper.*

Key Words: *centrifugal pump, innovative design, liquid hydrogen, CFD.*

1. INTRODUCTION

Depending on the mission nature, the shuttle (space vehicle) may be classified in several categories [1]. These include satellites orbiting around the Earth or around the Moon, interplanetary flights or unmanned vehicles. The propulsion of these shuttles is of two kinds [2], primary and secondary. In the primary type, the space vehicle aims to go on the calculated trajectory while the secondary refers to attitude control, rotation, gyroscopic discharges, the separation moment and so on. A propulsion mechanism provides the force that moves the bodies that are initially at rest by changing speed and surpassing all the forces that oppose the motion. Rocket propulsion systems can be classified [3] depending on the type of energy used (nuclear, solar or chemical), size, type of fuel, type of construction or the number of units used for spacecraft propulsion. A system for liquid rocket propulsion [4] requires valve precision and a complex mechanism of pumps; turbines or pressurized tanks and combustion chambers where the fuel is mixed with the oxidant and burned to form gas of high temperatures that will accelerate and achieve high speeds through a supersonic nozzle and propel the shuttle.

Liquid hydrogen is the fuel used to power most of the liquid rocket engines that equip spacecraft. Burning liquid hydrogen (LH2) in combination with liquid O2 yields a high

performance[5]. LH2 is an excellent regenerative coolant. In combination with O2, it burns with a colorless flame. However, the shock waves can be visible. Of all known fuels, LH2 is the lightest and with lower temperature, with a specific gravity of 0.07, and a boiling point around 20K. A low density propellant requires large tanks which lead to increased shuttle volume. Due to the very low temperatures of LH2, problems arise in the selection of materials for manufacturing both the tanks and the pipes. Also, to avoid liquid evaporation or condensation, isolating these tanks and pipelines is a particularly significant challenge.

The centrifugal pump is considered to be a kinetic device. The liquid enters the pump and receives kinetic energy from a rotating rotor. The centrifugal rotor sets the liquid up to high speeds to mechanically transfer the kinetic energy. Numerous researchers have made significant contributions to studying flow through these machines, all aiming at achieving the highest efficiency possible.

Studies by Eckardt [6], Johnson et al. [7], Kjork et al. [8], Denton [9], Dawes [10], Casey et al. [11], Bansod et al. [12], Krain et al. [13], Farge et al. [14] and Zhang et al. [15] represent significant efforts to study the flow in centrifugal rotors both numerically and experimentally. Recent, researchers like Hillewaert et al. [16], Gonzalez et al. [17-19], Byskov et al. [20], Meakhail et al. [21], Majidi [22] and Feng et al. [23] have tried to predict the performance of such a machine under different operating conditions.

Thus, numerous algorithms with main objective to numerically simulate the flow field in a centrifugal rotor have been developed. These algorithms are either pressure-based[24] or density-based [25] but both try on solve the Navier-Stokes equation system. Lakshminarayana [26], Rodi et al. [27] and Thakur et al. [28], have done a brief presentation of these techniques for assessing the performance of this machine type.

In this paper the literature was used to design a new centrifugal pump for LH2 (Liquid Hydrogen). To determine its performance, the CFD ANSYS-CFX commercial code was used.

2. THEORETICAL APPROACH

The design of a centrifugal pump starts from the desired operating conditions. Thus, the customer imposes the discharge pressure, the flow rate and the nature of the working fluid.

During the design process of a centrifugal pump for rocket engines, these important parameters are used:

- required pump mass flow,

$$Q = \rho v A \quad (1)$$

- required pump discharge pressure,

$$p_d = p_s + (\Delta p)_{pump} = p_1 + (\Delta p)_{drops} \quad (2)$$

- head,

The pressure increase generated by the pump between discharge and suction is named "head" and can be expressed as:

$$\Delta H = \frac{p_d + p_s}{\rho g} + Y_s + Y_d \quad (3)$$

- net positive suction head,

The NPSH can be divided into two types: the required NPSH (NPSH_r) and the available NPSH (NPSH_a). Both are pressure measurements expressed in meters. The NPSH_r is the

limit value of the head at the pump inlet that allows to avoid cavitation phenomena and The $NPSH_a$ measures the absolute pressure at the inlet.

$$NPSHa = H_{tank} \pm H_{elevation} H_{friction} H_{vapor} \quad (4)$$

To avoid pump cavitation $NPSHa > NPSHr$. [29]

- specific diameter,

The specific diameter is necessary to determine the impeller diameter and depends on the specific speed N_s .

$$D_s = \frac{D_2 (g\Delta H)^{1/4}}{\sqrt{Q}} \quad (5)$$

- impeller diameter,

$$D_2 = \frac{D_s \sqrt{Q}}{(g\Delta H)^{1/4}} \text{ or } D_2 = \frac{2u_2}{\omega} \quad (6)$$

- impeller-inlet velocity triangle, (Fig.1)

The inlet absolute velocity is:

$$c_1 = \frac{Q}{A_1} \quad (7)$$

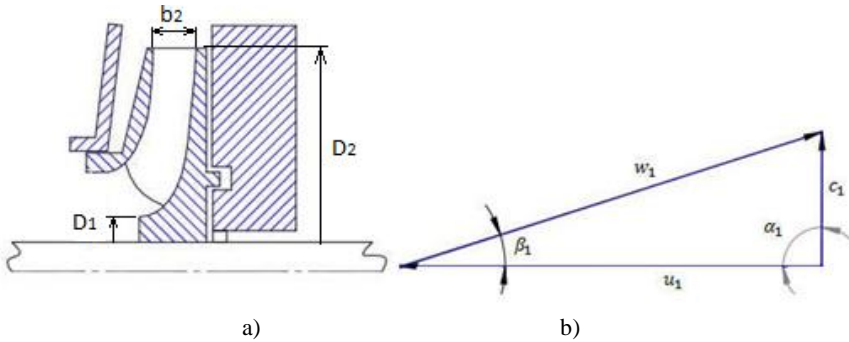


Figure 1: a) Centrifugal pump cross section, b) Inlet velocity triangle

$$u_1 = 2\pi N_r D_1 \quad (8)$$

$$w_1 = \frac{c_1}{\sin(\beta_1)} \quad (9)$$

- impeller-outlet velocity triangle, (Fig. 2)

For the velocity triangle at the impeller outlet, two conditions must apply simultaneously [30]:

a) The work must be equal to the theoretical head required by the machine;

b) The meridional component of the absolute velocity must guarantee the discharge of the mass flow.

$$L = c_2 u_2 \cos(\alpha_2) \quad c_1 u_1 \cos(\alpha_1) = c_2 u_2 \quad c_{1u} u_1 = \frac{g\Delta H}{\eta_y} \quad (10)$$

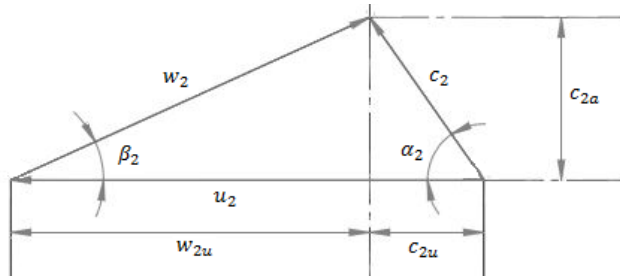


Figure 2: Impeller outlet velocity triangle

$$\left\{ \begin{array}{l} c_{2m} = \phi u_2 \\ c_2 = \sqrt{c_{2m}^2 + c_{2u}^2} \\ \beta_2 = \arctan\left(\frac{c_{2m}}{u_2 - c_{2u}}\right) \\ \alpha_2 = \arctan\left(\frac{c_{m2}}{c_{u2}}\right) = \arctan\left(\frac{\phi}{\frac{\psi}{\eta_y}}\right) \\ c_{2u} = \frac{u_2 \psi}{\eta_y} \\ w_2 = \sqrt{(c_2^2 + u_2^2) [2u_2 c_2 \cos(\alpha_2)]} \end{array} \right. \quad (11)$$

- number of blades,

$$Z = 6.5 \frac{D_2 + D_1}{D_2 - D_1} \sin(\beta_1 + \beta_2) \quad (12)$$

- blade height at the outlet,

$$b_2 = 0.78 \left(\frac{N_s}{100}\right)^{1/6} \sqrt[3]{\frac{Q}{n}} \quad (13)$$

- total pump efficiency,

$$\eta_p = \eta_Y \eta_V \eta_{Tr} \quad (14)$$

3. GEOMETRIC MODELS

Using the above parameters, a preliminary design of the new centrifugal impeller, rotor stage over stage was carried out, Fig. 3.

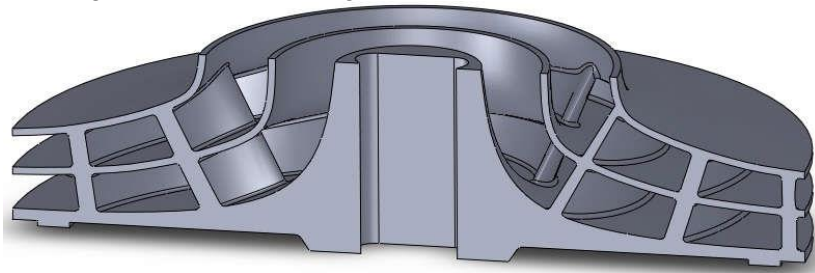


Figure 3: New Impeller stage-over-stage

The fluid path in this new pump design is explained in the figure 4. The LH₂ will enter first in the impeller, stage I (green arrow), and pass into the stator part (yellow arrow) to enter again in the impeller but in the stage II (red arrow). After these steps, the working fluid passes in the volute through the stator blades.

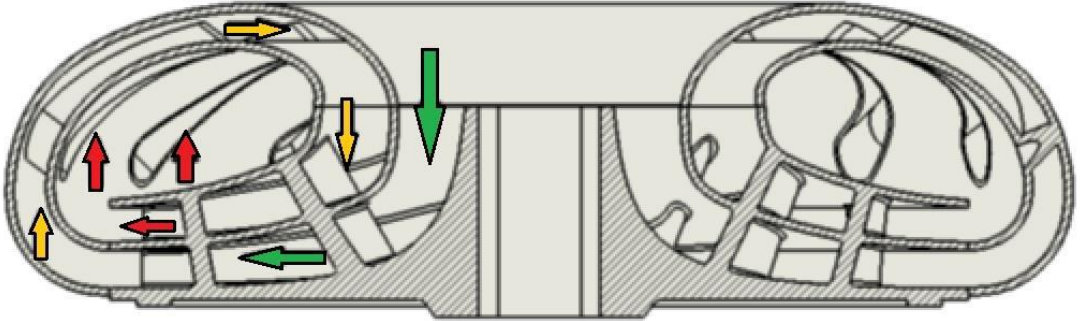


Figure 4: Path flow through the two stages of the innovative pump (green arrows inlet and first rotor; orange arrows first stator; red arrow second rotor and discharge)

By superposing the two stages of the LH₂ pump, the total length is minimized at the same diameter of the rotor.

Also, the discharge port can be configured as convenient for the integration into the fuel system since the pressure is evenly distributed into the volute and the flow can be directed towards the desired interface. In Fig. 5 there a cross section of this innovative pump assembly is presented.

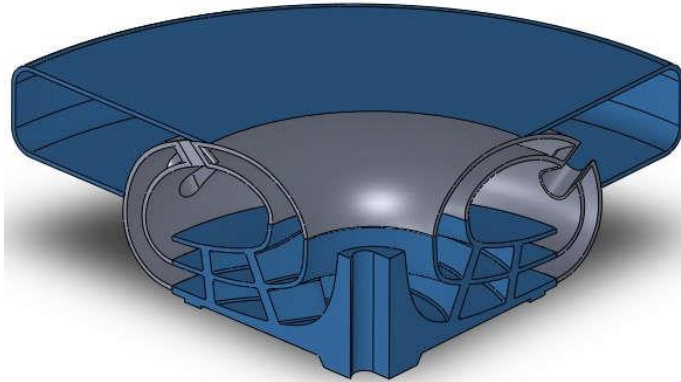


Figure 5: Cross section of the innovative pump assembly

4. CFD SIMULATION AND RESULTS

4.1 CFD setup

This study is based on numerical methods used to determine centrifugal pump hydrodynamic performances.

To establish the optimal configuration in-house codes, developed by the authors, were used [31].

In this way, a series of configurations with different main working parameters has been considered.

Such modified parameters were blade profiles, number of blades, solidity factor and so on.

Once these configurations were determined, a CFD analysis was carried out to assess the hydrodynamic performances. Fig. 6 shows the work flow of the approach.

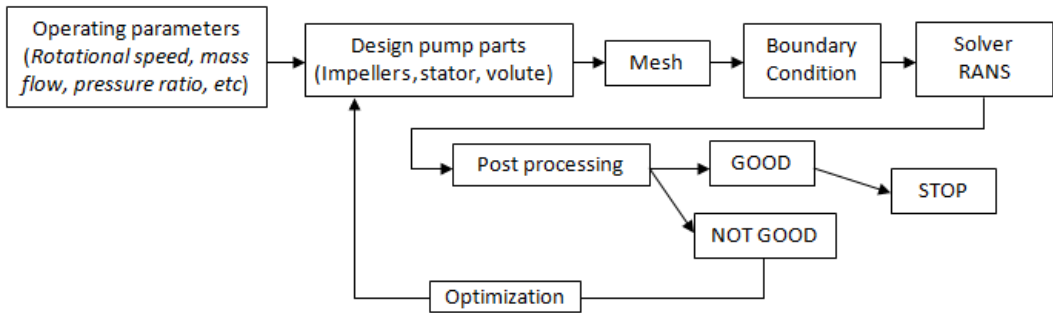


Figure 6: Workflow

The CFD analyses were performed on 3D domains. The numerical solvers used are pressure based and use the SIMPLE method [32].

The commercial code ANSYS-CFX [33] with RANS solver and the k- ω SST turbulence model [34] was used.

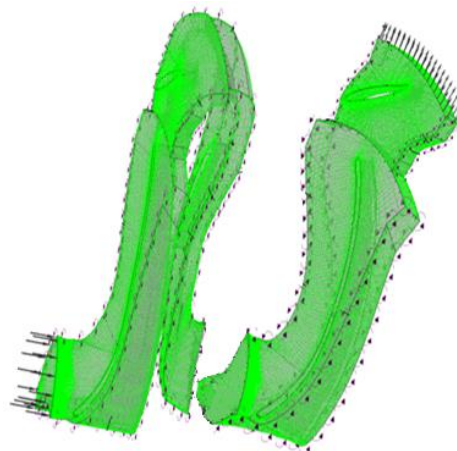
$$\left\{ \begin{array}{l} \frac{\partial k}{\partial t} + \bar{u} \frac{\partial k}{\partial x} + \bar{v} \frac{\partial k}{\partial y} + \bar{w} \frac{\partial k}{\partial z} = \Gamma_k \left(\frac{\partial^2 k}{\partial x^2} + \frac{\partial^2 k}{\partial y^2} + \frac{\partial^2 k}{\partial z^2} \right) + \tilde{G}_k - Y_k \\ \frac{\partial \omega}{\partial t} + \bar{u} \frac{\partial \omega}{\partial x} + \bar{v} \frac{\partial \omega}{\partial y} + \bar{w} \frac{\partial \omega}{\partial z} = \Gamma_\omega \left(\frac{\partial^2 \omega}{\partial x^2} + \frac{\partial^2 \omega}{\partial y^2} + \frac{\partial^2 \omega}{\partial z^2} \right) + G_\omega - Y_\omega + D_\omega \end{array} \right. \quad (15)$$

The discretization domain was divided in three sub-domains. Two of them were rotating domains, which include the blades of the impeller, and the third sub-domain was a stationary domain that represents the stator part.

The domain discretization was done by using dedicated grid generators like TurboGrid and ICEM CFD.

To control the boundary layer and to reduce the time necessary to reach convergence, the meshes were of structured type.

In Fig. 7 the boundary conditions for the two included cases are presented, the classic configuration with two stages and the newly proposed configuration, with stage-over-stage.



a)

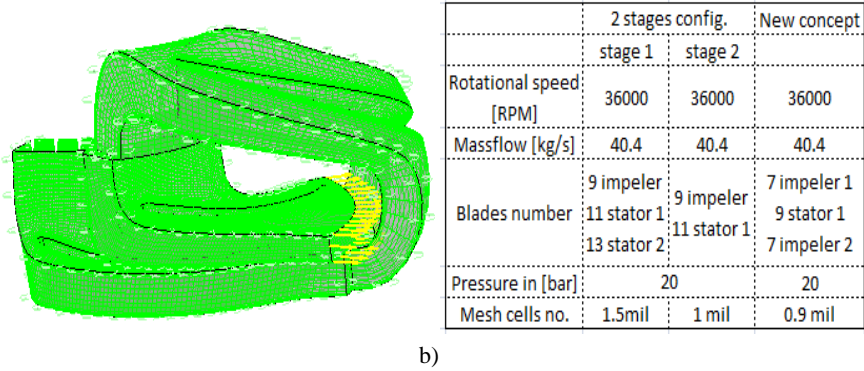


Figure 7: Boundary condition for: a) classic two stages pump; b) stage-over-stage pump

4.2 Results

In order to investigate in detail the performance of this new centrifugal pump concept, steady CFD analysis was performed and the results were compared the CFD data from a simulation of a two stages centrifugal pump.

Fig. 8 shows the streamlines at 50% blade span for these two cases. It can be observed that there is a small recirculation zone on the stator blade, but even with that, the efficiency of this new concept is better than for a classic pump, see Table 1.

Regarding the pressure distribution, in Fig. 9 is presented the pressure in the same plane as the streamlines, and in Fig. 10 is represented the pressure variation from inlet to outlet.

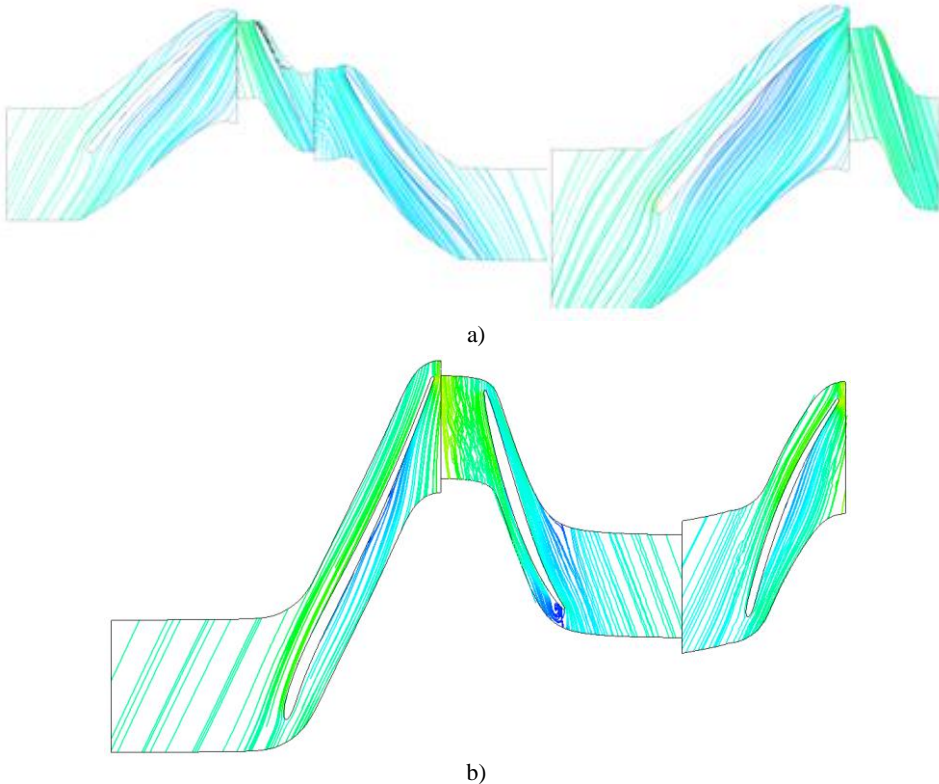


Figure 8: Streamlines: a) classic two stages pump; b) stage-over-stage pump

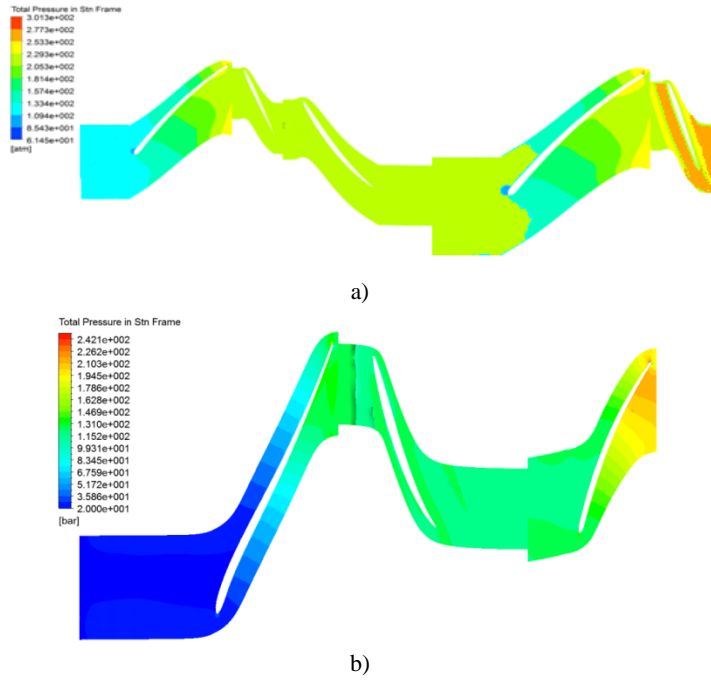


Figure 9: Total pressure in Stn Frame counters: a) classic two stages pump; b) stage-over-stage pump

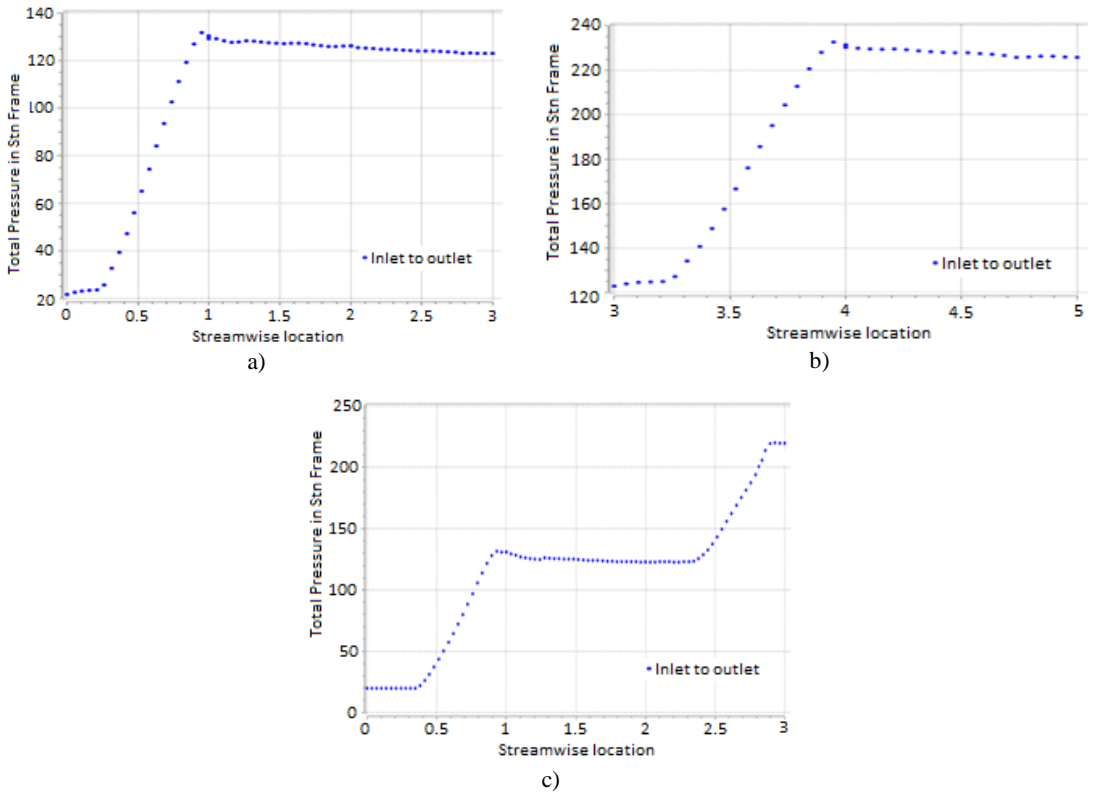


Figure 10: Total pressure variation from inlet to outlet: a) first stage of a classic two stages pump; b) second stage of a classic two stages pump; c) stage-over-stage pump

Table 1: CFD-results of the centrifugal pumps cases

	Quantity	Inlet	Outlet	Ratio (Out/In)
Stage 1 classic config.	Pressure	1.807e+006 kg m ⁻¹ s ⁻²	1.09453e+007 kg m ⁻¹ s ⁻²	6.0571
	Total Pressure	2.16424e+006 kg m ⁻¹ s ⁻²	1.24484e+007 kg m ⁻¹ s ⁻²	5.7518
	Efficiency From Power		0.866	
Stage 2 classic config.	Pressure	1.21478e+007 kg m ⁻¹ s ⁻²	2.08993e+007 kg m ⁻¹ s ⁻²	1.72042
	Total Pressure	1.24424e+007 kg m ⁻¹ s ⁻²	2.28756e+007 kg m ⁻¹ s ⁻²	1.83852
	Efficiency From Power		0.876	
New concept pump	Pressure	1.76439e+006 kg m ⁻¹ s ⁻²	1.73325e+007 kg m ⁻¹ s ⁻²	9.823508408
	Total Pressure	1.99604e+006 kg m ⁻¹ s ⁻²	2.518e+007 kg m ⁻¹ s ⁻²	12.61497766
	Efficiency From Power		0.883	

5. CONCLUSIONS

The purpose of this study was to numerically determine the efficiency of a new LH2 centrifugal pump design. This turbomachine can be used for space shuttle propulsion. All simulations were done in a 3D setup using the SST turbulence model, which can capture very well the flow near walls. The total pressure distribution for the two stages configuration and the stage-over-stage cases are presented. Also, the efficiency was determined in this study. By using the new geometry, the axial length is decreased by 60 % and the weight by 30% compared to a classic two stage configuration.

REFERENCES

- [1] * * * Encyclopedia Astronautica, *Shuttle*, Archived from original, January 18, 2010.
- [2] * * * Glenn Research Center, *In-space propulsion program*, NASA, 2013.
- [3] G. P. Sutton, O. Biblarz, *Rocket propulsion elements*, Wiley interscience, ISBN 0-471-32642-9, 2000.
- [4] G. P. Sutton, History of liquid propellant rocket engines in the united states, *Jornal of Propulsion and Power*, **19**(6), 978-1007, 2003.
- [5] P. Folly, P. Mader; Propellant Chemistry, *Chimia international journal for Chemistry*, Volume **58**, number 6, pp. 374-382(9), 2004.
- [6] D. Eckardt, Detailed flow investigations within a high-speed centrifugal compressor impeller, *ASME Journal of Fluids Engineering*, vol. **98**, pp. 390-402, 1976.
- [7] M. W Johnson, J. Moore, The development of wake flow in a centrifugal impeller, *ASME Journal of Engineering for Power*, vol. **102**, pp. 382-390, 1980.
- [8] A. Kjork, L. Lofdahl, Hot-wire measurement inside a centrifugal impeller, *ASME Journal of Fluids Engineering*, vol. **111**, pp. 363- 368, 1989.
- [9] J. D. Denton, The calculation of three-dimensional viscous flow through multistage turbomachinery, *ASME Journal of Turbomachinery*, vol. **114**, pp. 18-26, 1992.
- [10] M. W. Dawes, Toward improved through flow capability: the use of three-dimensional viscous flow solvers in a multistage environment, *ASME Journal of Turbomachinery*, vol. **114**; pp. 8-17, 1992.
- [11] M. V. Casey, P. Dalbert, P. Roth, The use of 3D viscous flow calculations in the design and analysis of centrifugal compressors, *ASME Journal of Turbomachinery*, vol. **114**, pp. 27-37, 1992.
- [12] P. Bansod, C. M. Rhie, *Computation of flow through a centrifugal impeller with tip leakage*, AIAA Paper No 90-2021, 1990.
- [13] H. Krain, W. Hoffman, *Verification of an impeller by laser measurement and 3D viscous flow calculations*, ASME Paper 89-GT-150, 1989.
- [14] T. Z. Farge, M. W. Johnson, *The effect of backswept blading on the flow in a centrifugal compressor impeller*, ASME Paper 90-GT-231, 1990.
- [15] M. J. Zhang, C. G. Gu, Y. M. Miao, *Numerical study of the internal flow field of a centrifugal impeller*, ASME Paper 94-GT-357, 1994.

- [16] K. Hillewaert, R. A. Van den Braembussche, Numerical simulation of impeller-volute interaction in centrifugal compressors, *ASME Journal of Turbomachinery*, vol. **121**, pp.603-609, 1999.
- [17] J. Gonzalez, J. Fernandez, E. Blanco, C. Santolaria, Numerical simulation of the dynamic effects due to impellervolute interaction in a centrifugal pump, *ASME Journal of Fluids Engineering*, vol. **124**, pp. 348-355, 2002.
- [18] J. Gonzalez, J. Parrondo, C. Santolaria, E. Blanco, Steady and unsteady forces for a centrifugal pump with impeller to tongue pump variation, *ASME Journal of Fluids Engineering*, vol. **128**, pp. 454-462, 2006.
- [19] J. Gonzalez, C. Santolaria, Unsteady flow structure and global variables in a centrifugal pump, *ASME Journal of Fluids Engineering*, vol. **128**, pp. 937-946, 2006.
- [20] R. K. Byskov, C. B. Jacobsen, N. Pedersen, Flow in a centrifugal pump impeller at design and off-design conditions-Part II: Large Eddy Simulations, *ASME Journal of Fluids Engineering*, vol. **125**, pp. 73-83, 2003.
- [21] T. Meakhail, S. O. Park, A study of impeller-diffuser-volute interaction in a centrifugal fan, *ASME Journal of Turbomachinery*, vol. **127**, pp. 84-90, 2006.
- [22] K. Majidi, Numerical study of unsteady flow in a centrifugal pump, *ASME Journal of Turbomachinery*, vol. **127**, pp. 363-371, 2005.
- [23] J. Feng, F. K. Benra, H. J. Dohmen, Numerical investigation on pressure fluctuations for different configurations of vaned diffuser pumps, *International Journal of Rotating Machinery*, 2007.
- [24] H. Montazeri, J. Mostaghimi, Interfacial Forces and Pressure-Based Algorithms, *Conference: 19th AIAA Computational Fluid Dynamics*, DOI: 10.2514/6.2009-3889, 2009.
- [25] V. SWare, H. N. Bharathi, Study of Density based Algorithms, *International Journal of Computer Applications*, **69**(26), DOI: 10.5120/12132-8235, 2013.
- [26] B. Lakshminarayana, An assessment of computational fluid dynamic techniques in the analysis and design of turbomachinery, *ASME Journal of Fluids Engineering*, vol. **113**; pp. 315-352, 1991
- [27] W. Rodi, et. All., Finite volume methods for two-dimensional incompressible flows with complex boundaries, *Computer Methods in Applied Mechanics and Engineering*, vol. **75**, pp. 369-392,1989.
- [28] S. Thakur, et. All., Development of pressure-based composite multigrid methods for complex fluid flows, *Program in Aerospace Science*, vol. 32, pp. 313-375, 1996.
- [29] J. Pei, et all., Cavitation optimization for a centrifugal pump impeller by using orthogonal design of experiment, *Chinese Journal of Mechanical Engineering*, **30**(1):103-10, DOI: 10.3901/CJME.2016.1024.125, 2017.
- [30] P. M. Singh, et all., Hydrodynamic performance of a pump-turbine model in the “S” characteristic region by CFD analysis, *Journal of the Korean Society of Marine Engineering*, Vol. **39**, No. 10 pp. 1017~1022, 2015.
- [31] R. Mihalache, et. All., Advanced Strategic Planning and Capability Identification in Order to Develop a Liquid Hydrogen Turbopump, *Applied Mechanics and Materials*, Vol. **555**, pp. 66-71,2014.
- [32] C. Schubert, et all., *Process Model Development for Reheating Plants using simple Numerical Methods enhanced with CFD Results*, 3rd European Steel Technology & Application Days (ESTAD), At Vienna, Austria, 2017.
- [33] * * * Ansys – Fluent, User guide, 2014.
- [34] G. Kalitzin, G. Medic, G. Iaccarino, P. Durbin, Near-wall behavior of RANS turbulence models and implications for wall functions, *Journal of Computational Physics*, **204**, pp. 265–291, 2005.